Fatigue Behavior of Al-Si-Cu-Mg Casting Alloys

Qigui Wang and Peggy Jones
Advanced Materials
GM - Powertrain

Background

- Application of Al-Si-Cu-Mg Casting Alloys
  - Complex engine components because of reasonable castability, good high temperature mechanical properties, and low cost compared with other primary alloys
  - Concerns of fatigue resistance
- Objectives
  - To study the influence of Sr, grain refinement with “TiBloy”, and low pressure filling on fatigue;
  - To determine weak links that controls fatigue, and
  - To develop microstructure tolerant design (MTD) method based on statistics and fracture mechanics.

Experimental

- Alloy (319)

Chemistry (wt%)	SPECIFIC GRAVITY (g/cc)	Si	Cu	Fe	Mn	Mg	Ti	Sr	Mn:Fe Ratio
Base	2.68	6.86	3.26	0.17	0.059	0.31	0.091	0.0005	0.42
Base +TiB2	2.67	6.96	3.27	0.21	0.086	0.31	0.100	0.0008	0.55
Sr	2.67	7.01	3.20	0.19	0.068	0.29	0.091	0.0151	0.49
Sr+TiB2	2.68	7.03	3.30	0.20	0.079	0.30	0.101	0.0194	0.54
LP Base	2.68	6.66	3.26	0.20	0.048	0.31	0.102	0.0002	0.24

- Test castings of cylinder heads were lost foam cast using both gravity pouring and low pressure fill.
- T7 heat treatment including solution treatment for 12 hr at 493°C, Quenching into agitated warm water (70°C), and artificial aging for 8 hr at 249°C.
- Both tensile and fatigue specimens were prepared and tested at room temperature at WMT&R per ASTM E466.

Experimental

- Metallography
  - – Porosity: vol%, maximum Feret diameter, area
  - – Dendrite cell size (DCS): a circle grid (5 circles) used
- Fractography
  - – Fatigue crack origin;
  - – Initial crack (pore/oxide) size; and
  - – Weak links controlling crack propagation

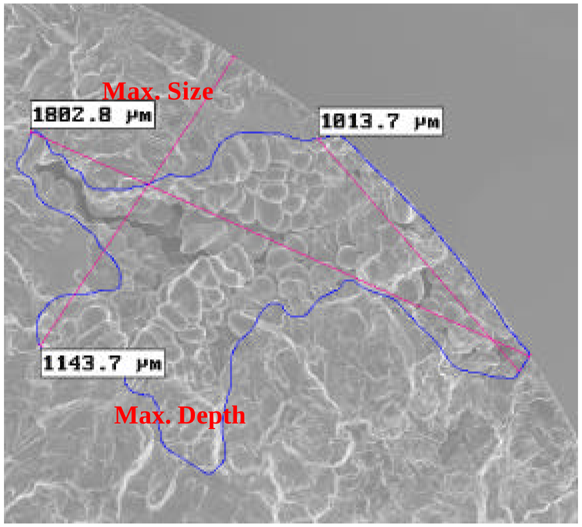

Microstructure

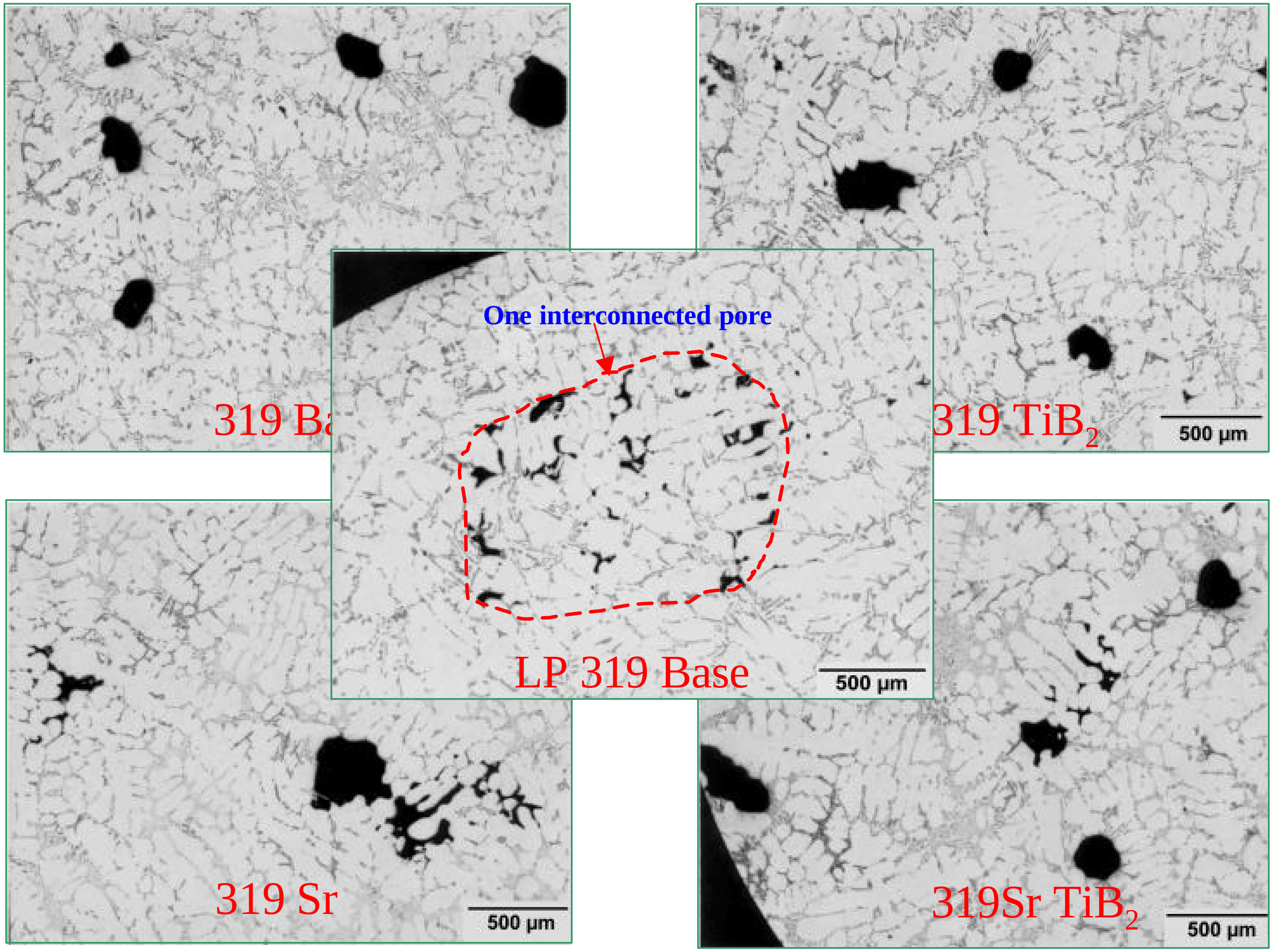

Microstructure (Grain Structure)

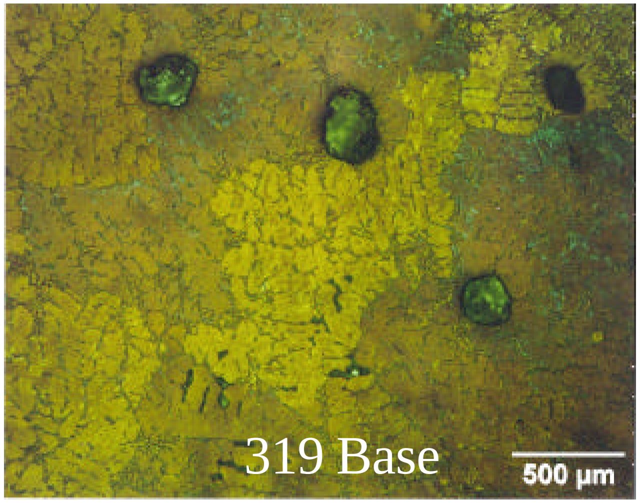

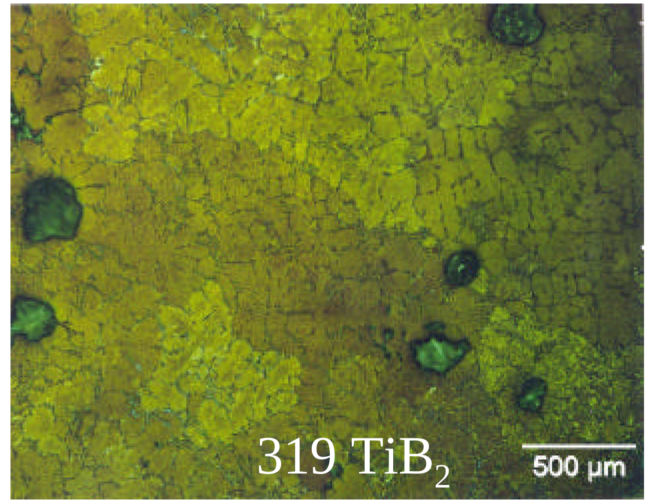

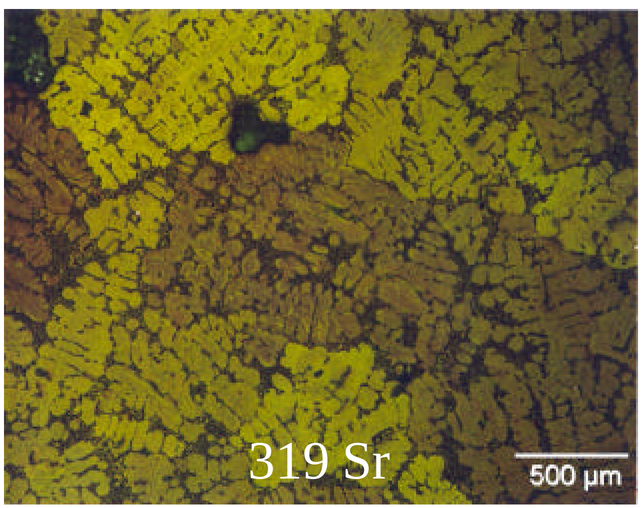

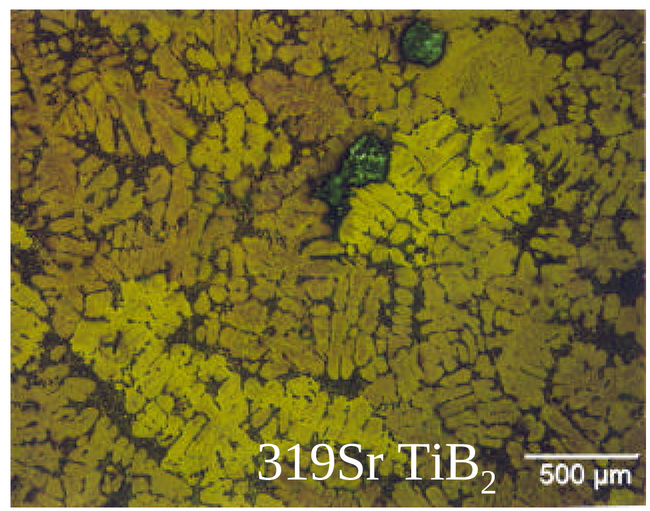

Microstructure Characterization

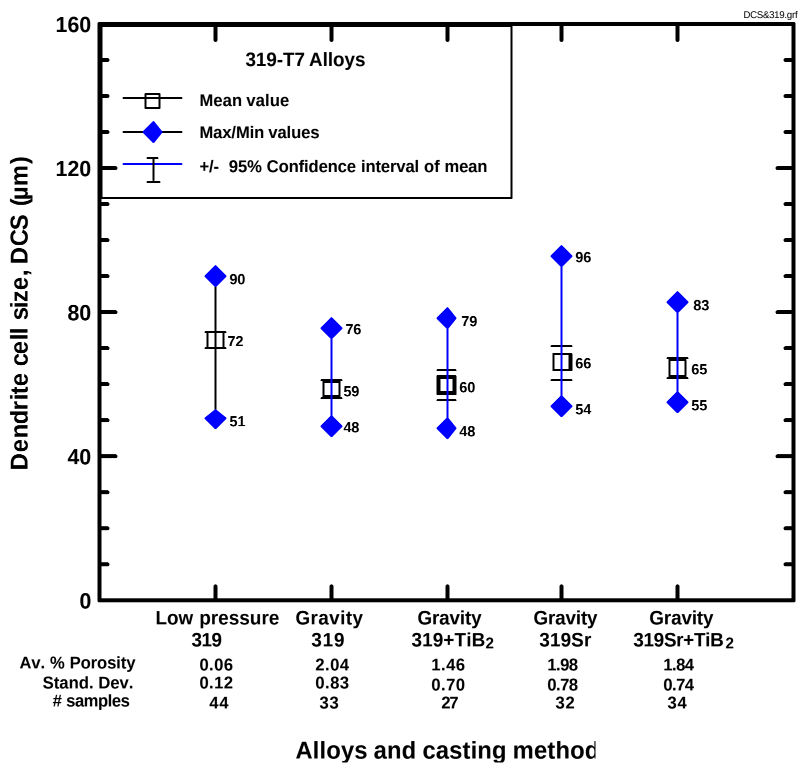

Dendrite Cell Size (DCS) vs. Alloys

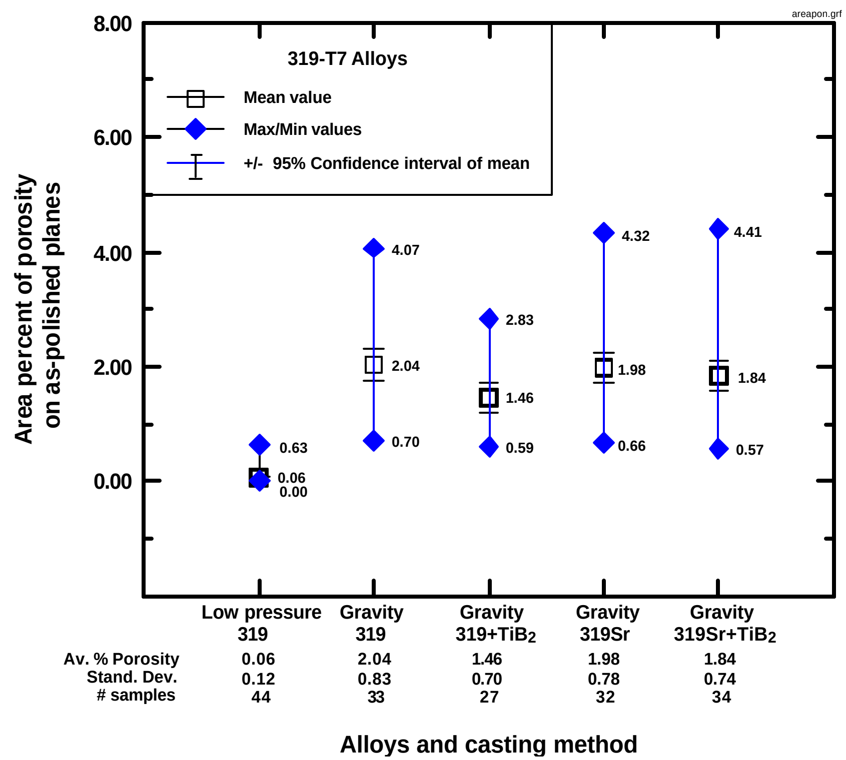

Porosity vs. Alloys

Microstructure Characterization

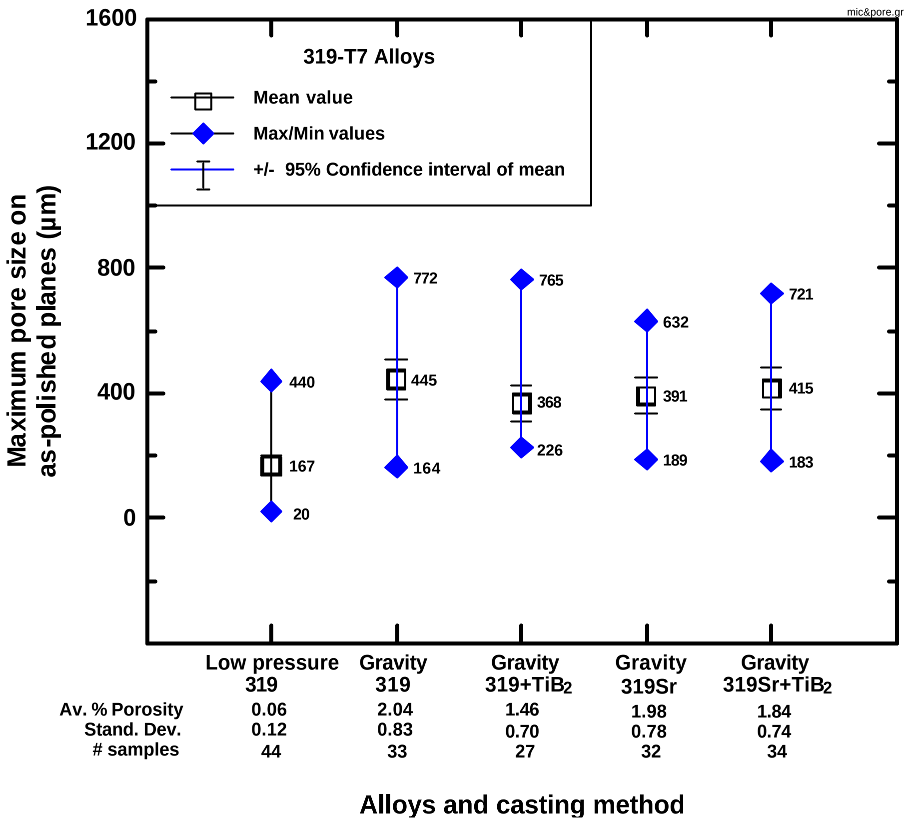

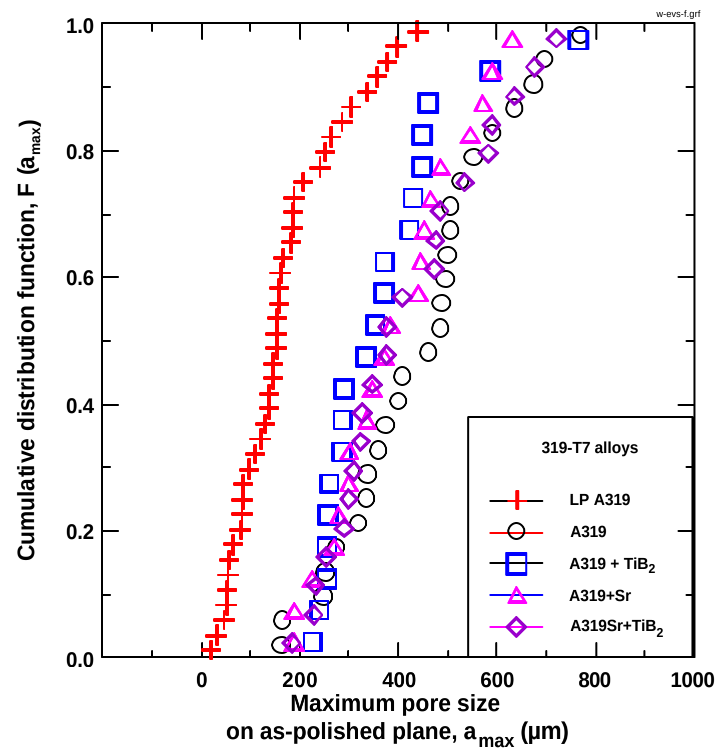

Maximum Pore Size vs. Alloys

Fatigue Crack Initiation and Propagation

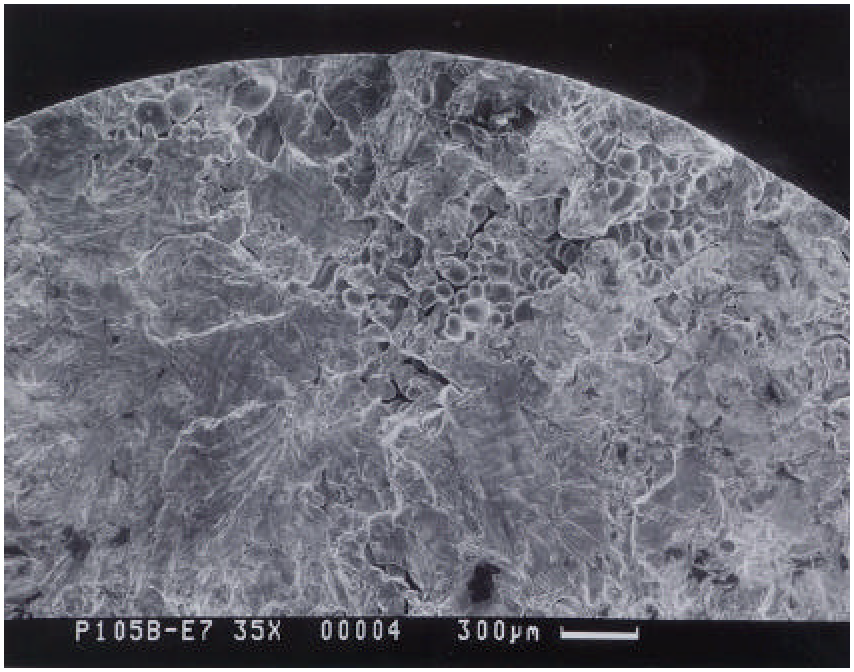

SEM fractograph

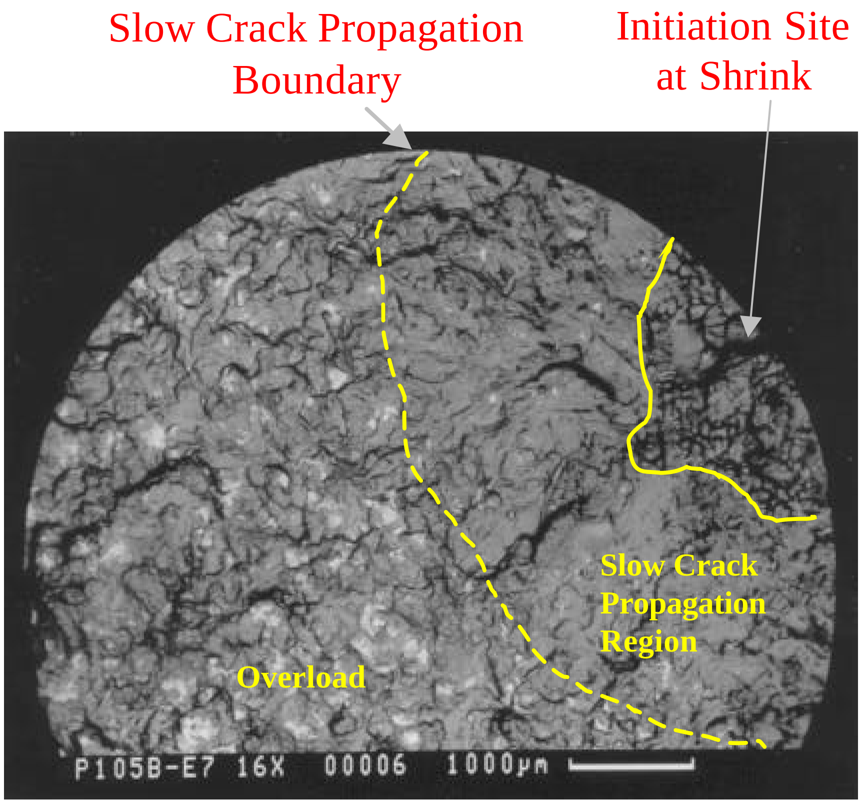

BEI fractograph

Shrinkage porosity initiated fatigue crack in a HCF specimen (LP 319 Base)
which failed after 1,666,452 cycles at 60MPa

Fatigue Crack Initiation and Propagation

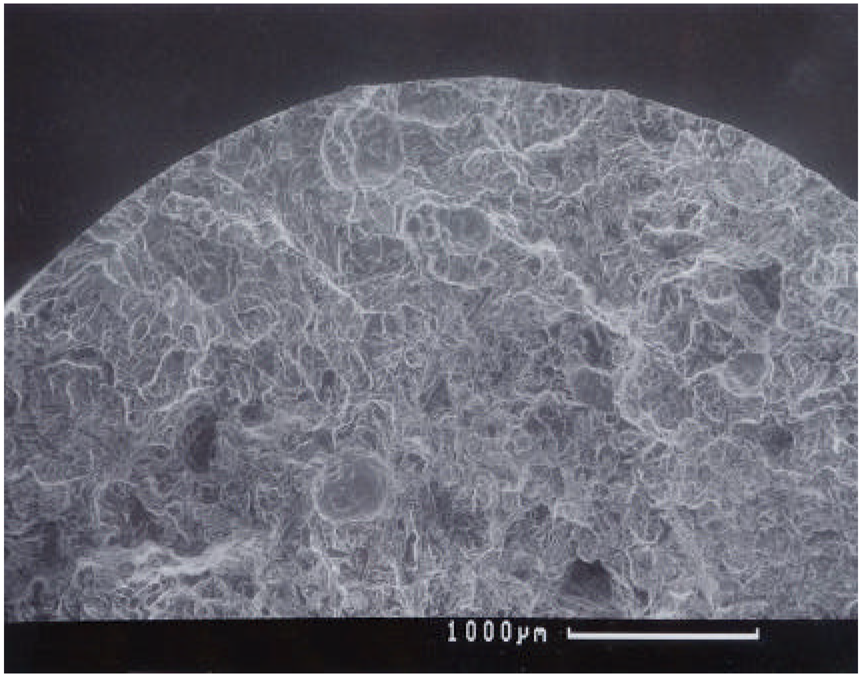

SEM fractograph

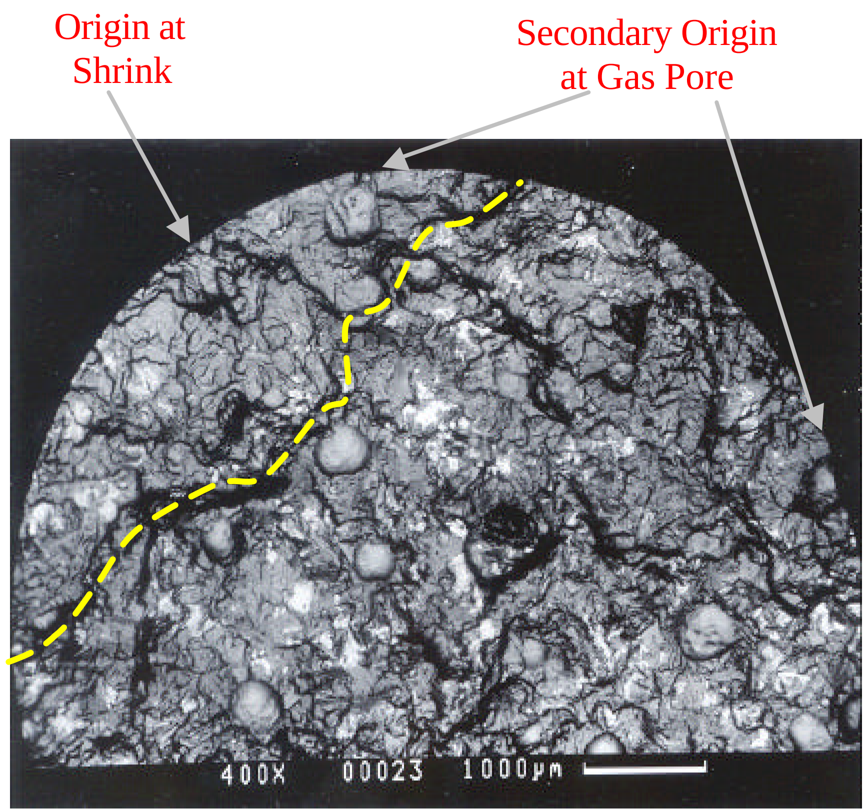

BEI fractograph

Shrinkage porosity initiated fatigue crack in a LCF specimen (319 Base)
which failed after 6,869 cycles at 145.5MPa

Fatigue Crack Initiation and Propagation

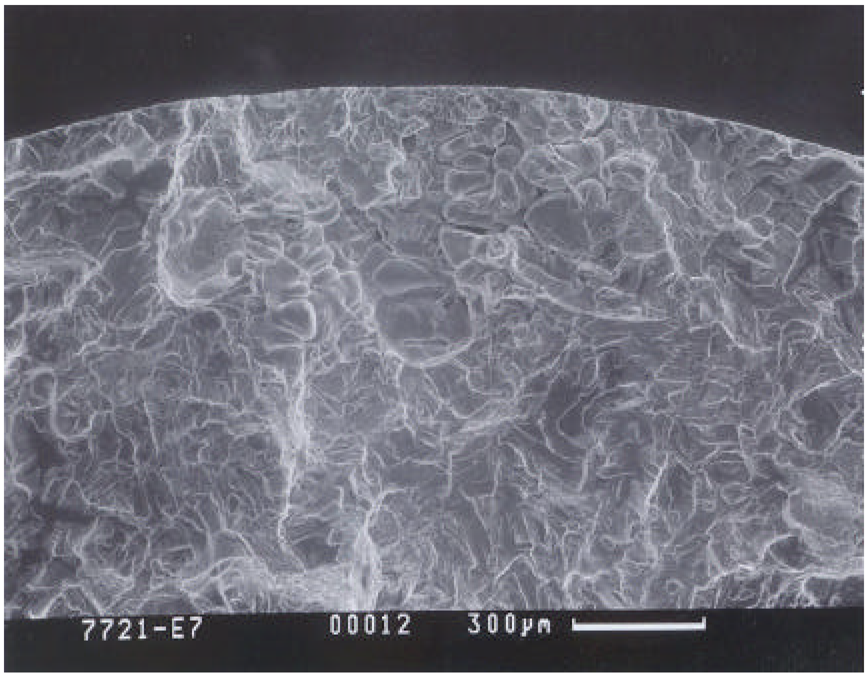

SEM fractograph

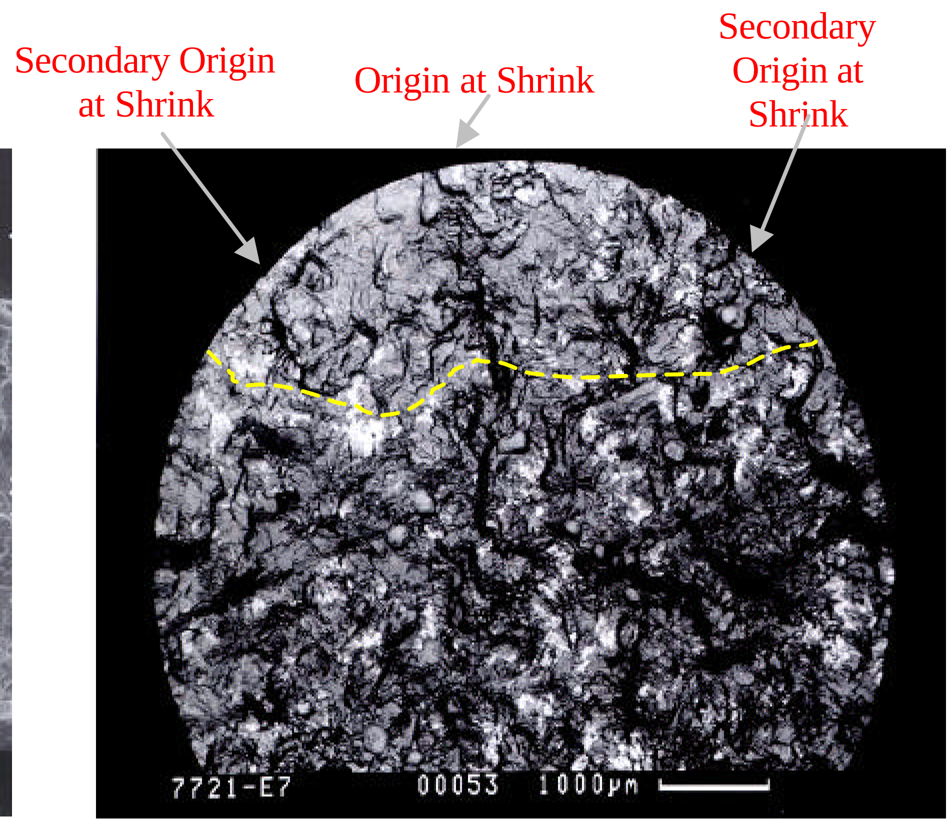

BEI fractograph

Shrinkage porosity initiated fatigue crack in a LCF specimen (319 TiB_2)
which failed after 3,156 cycles at 144MPa

Fatigue Crack Initiation and Propagation

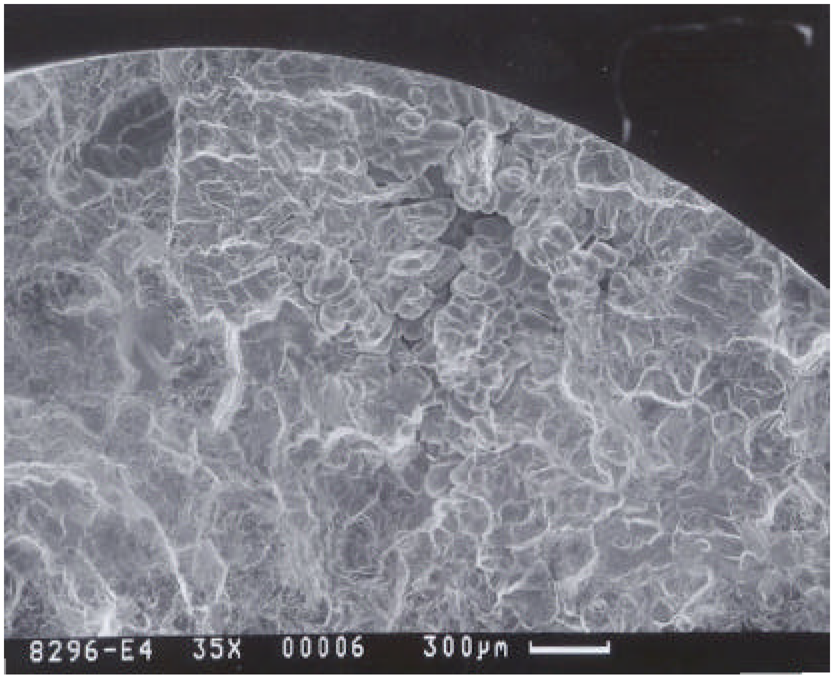

SEM fractograph

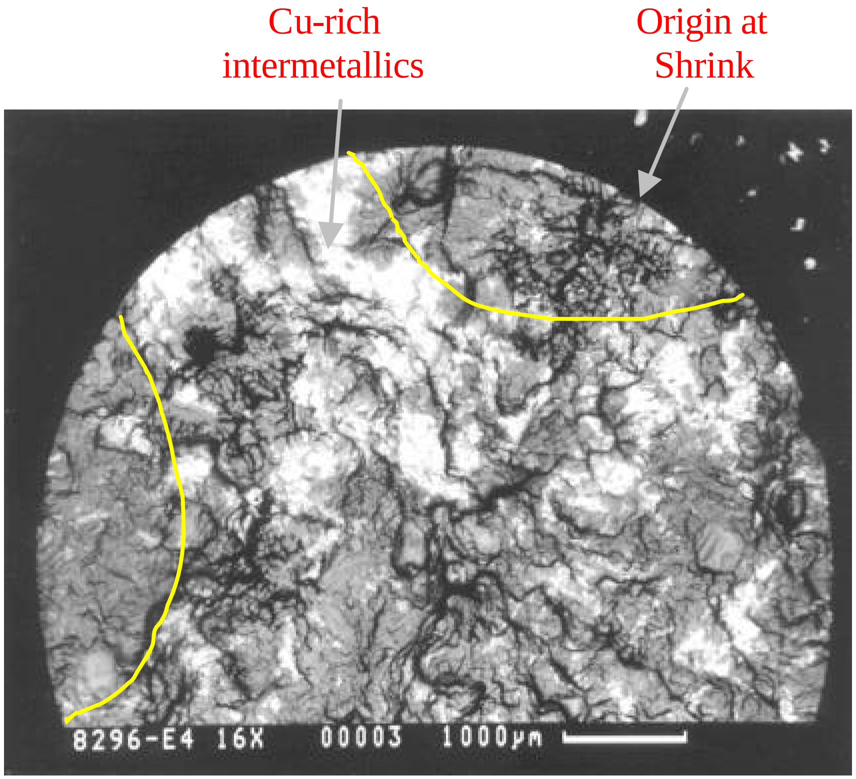

BEI fractograph

Shrinkage porosity initiated fatigue crack in a LCF specimen (319 Sr)
which failed after 3,609 cycles at 138MPa

Fatigue Crack Initiation and Propagation

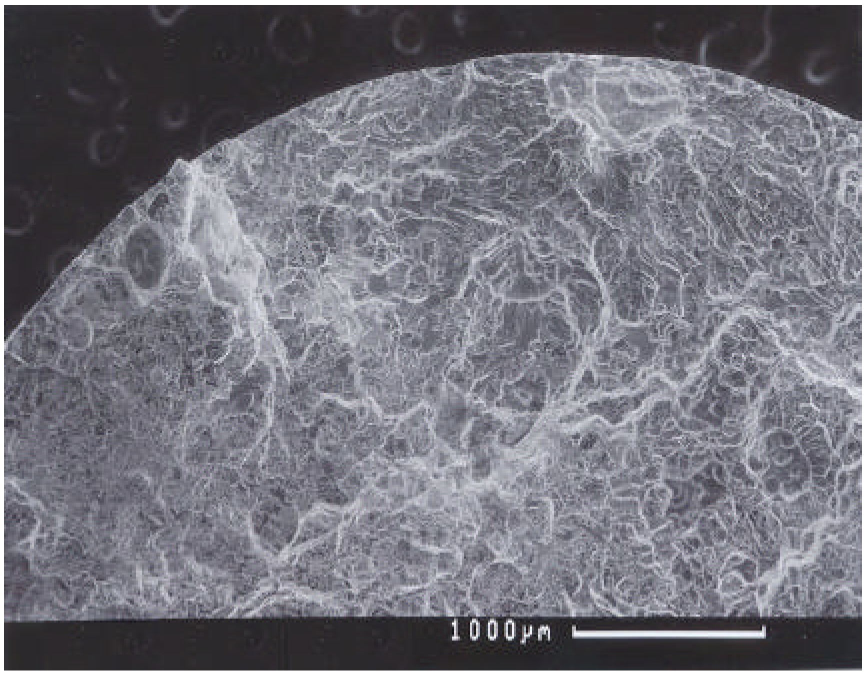

SEM fractograph

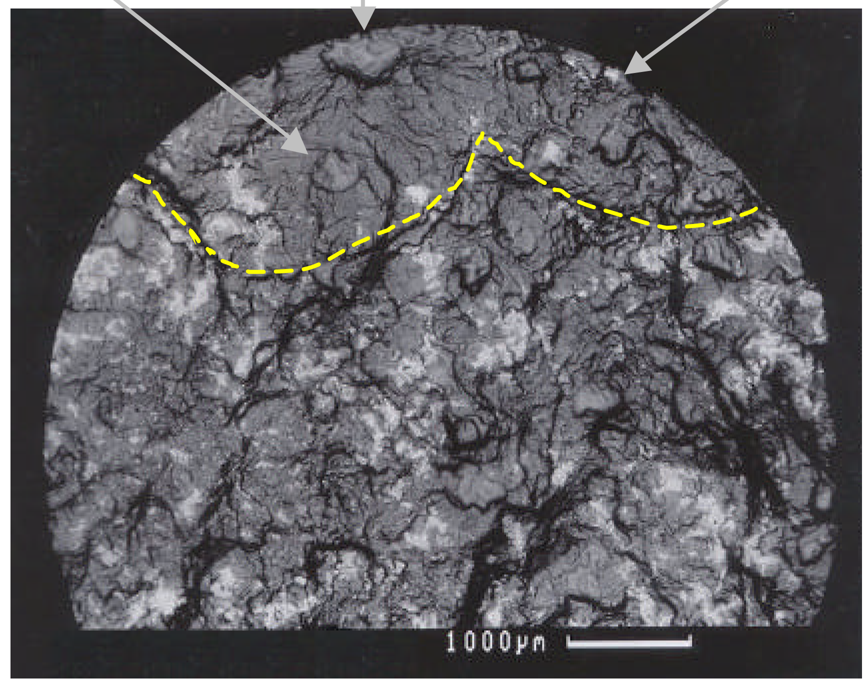

BEI fractograph

Shrinkage porosity initiated fatigue crack in a LCF specimen (319Sr+TiB_2)
which failed after 7,369 cycles at 150MPa

Fatigue Strength vs. Micros and Tensile (LCF)

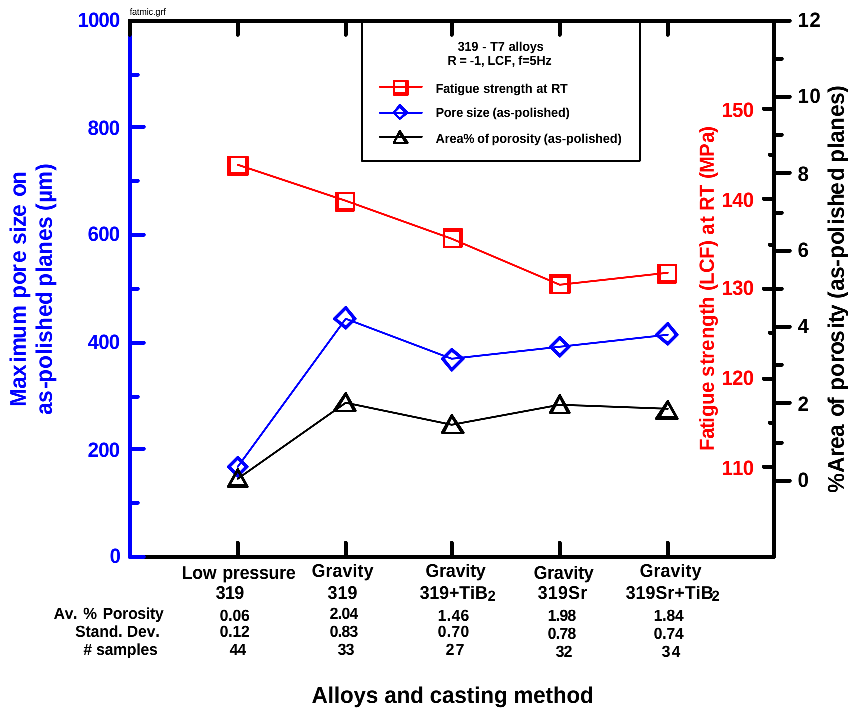

No clear relationship between fatigue properties and micros

No strong relationship between fatigue and tensile ductility for *T7*

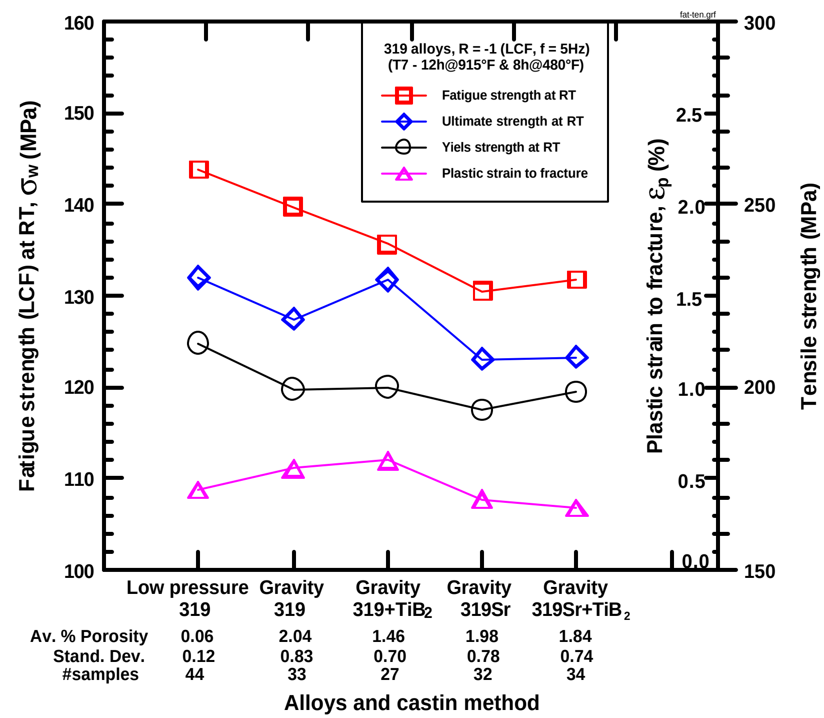

Comparison of Pore Sizes

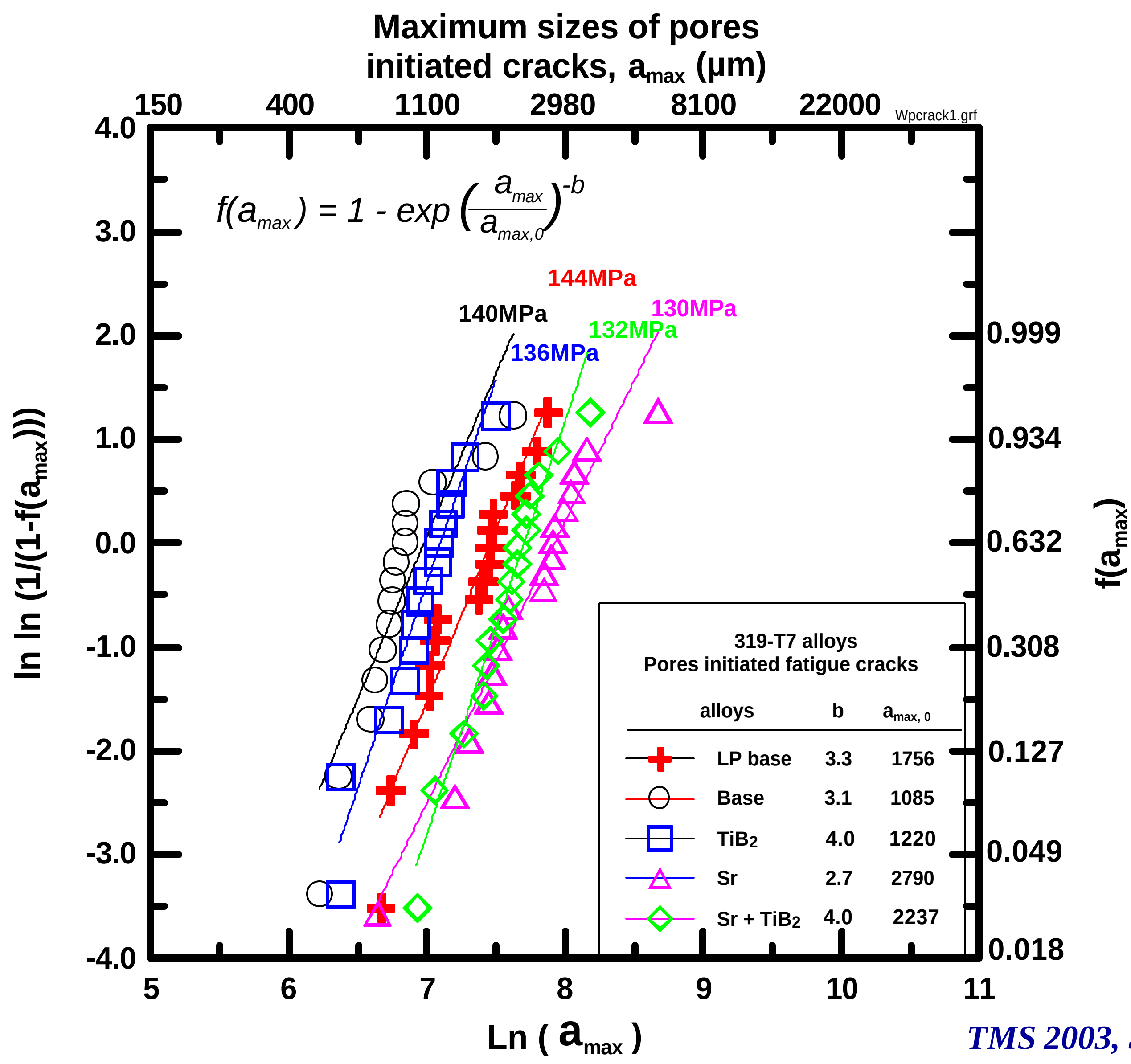

Weak Links and Fatigue Properties

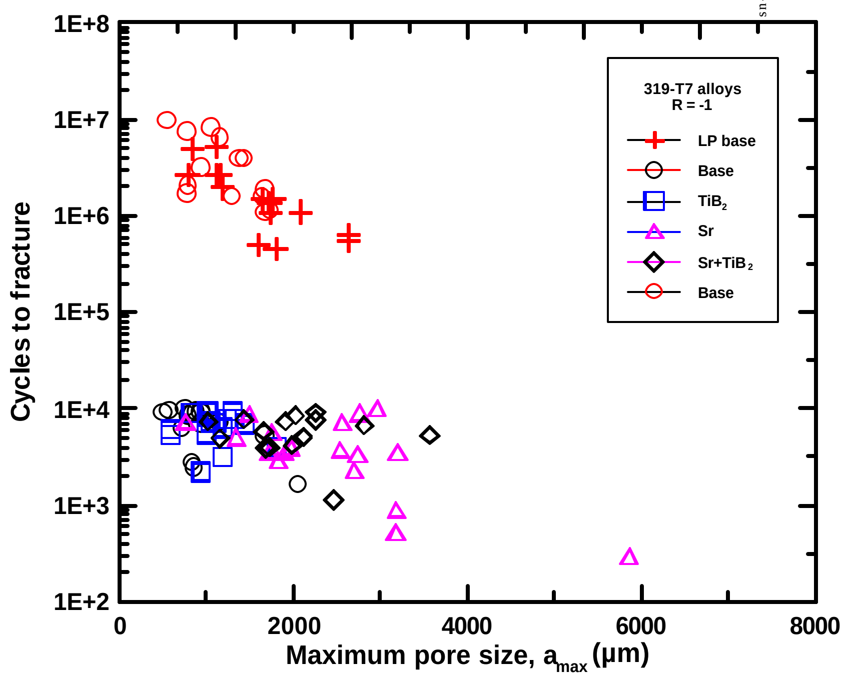

Good correlation between fatigue life and maximum pore size

Strong correlation between fatigue strength and area% of porosity and intermetallics on fracture surface

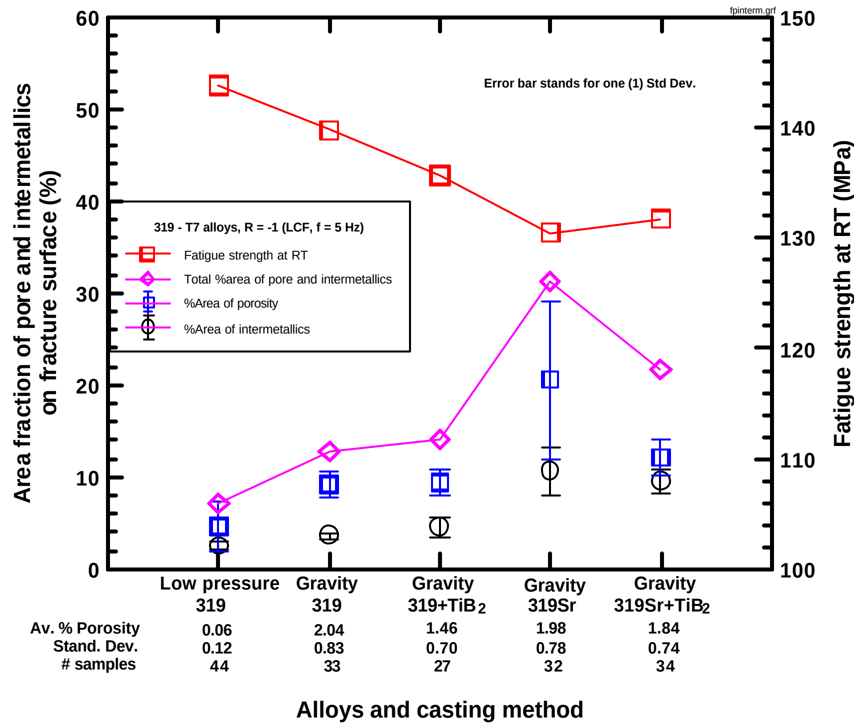

Microstructure Tolerant Design (MTD)

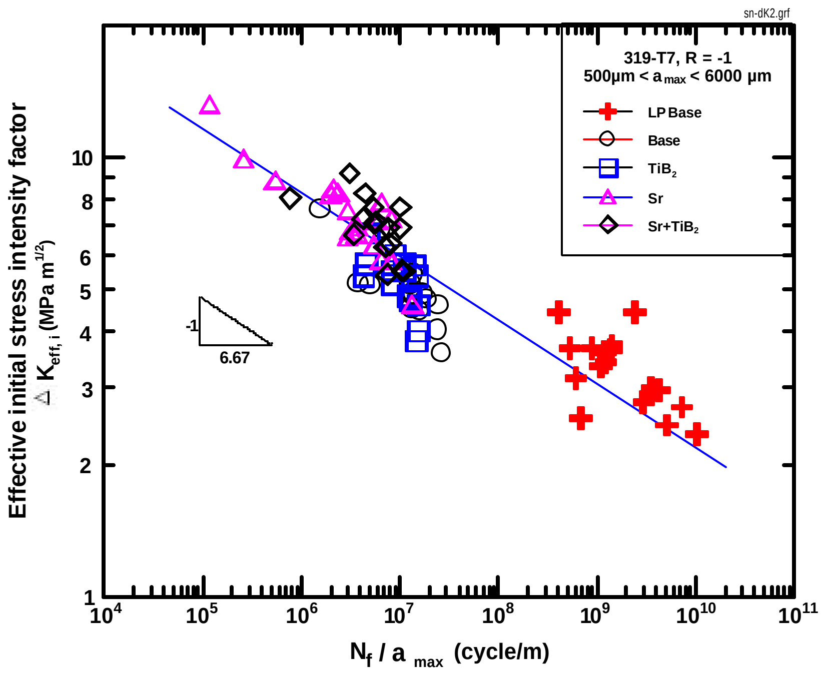

For applications

$N_f > 10^7$ cycles

Initial effective stress intensity factor range

$$\Delta K_{eff,i} = C \cdot \left({N_p}/{a_i} \right)^{-1/m}$$

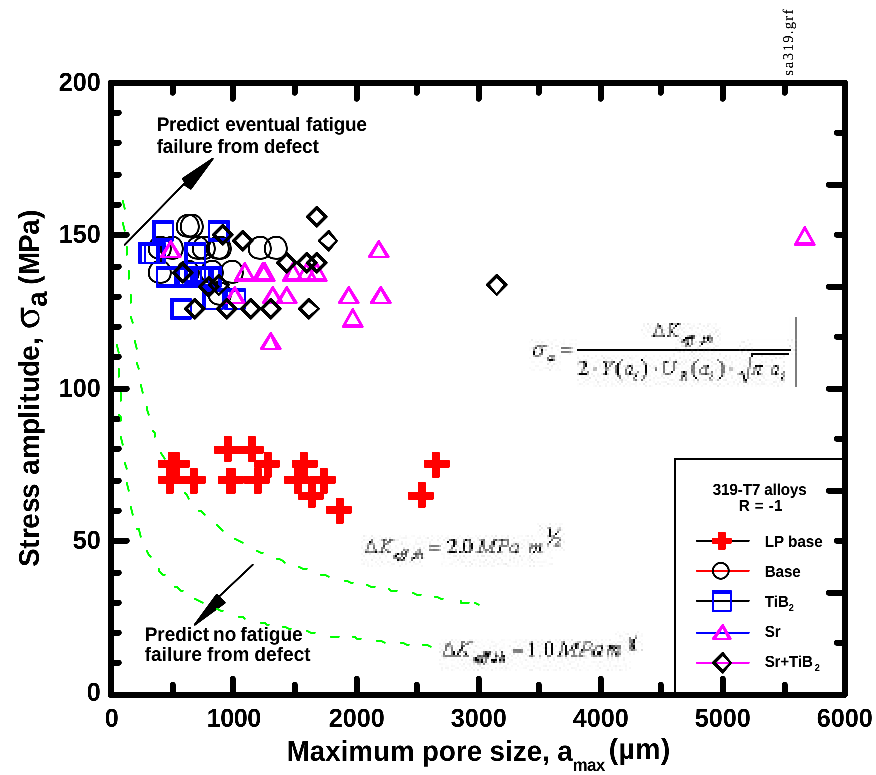

Microstructure Tolerant Design (MTD)

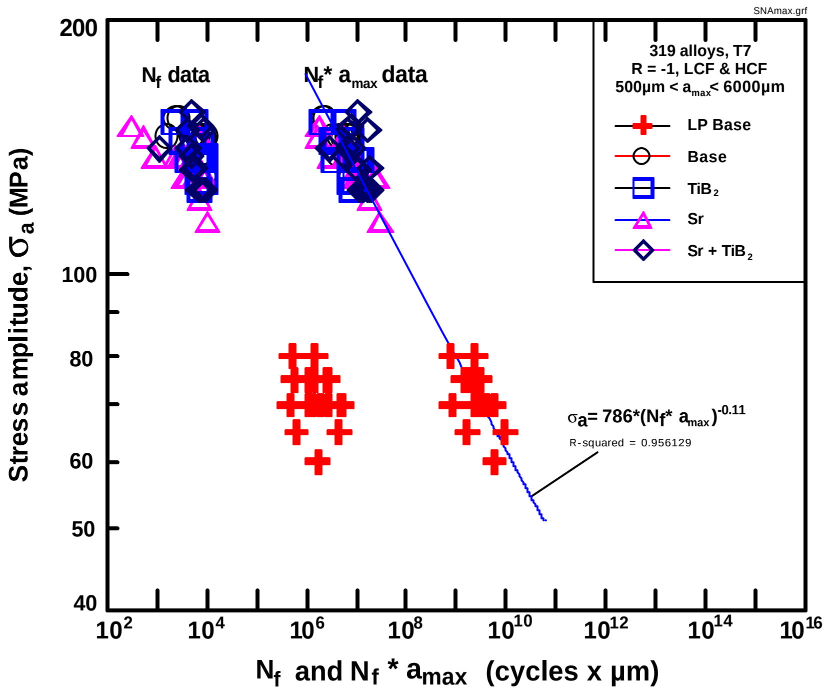

Long crack model

$$N_p = \frac{1}{a_i} \cdot \left(\frac{C}{s_a} \right)^m$$

For applications

$N_f < 10^7$ cycles

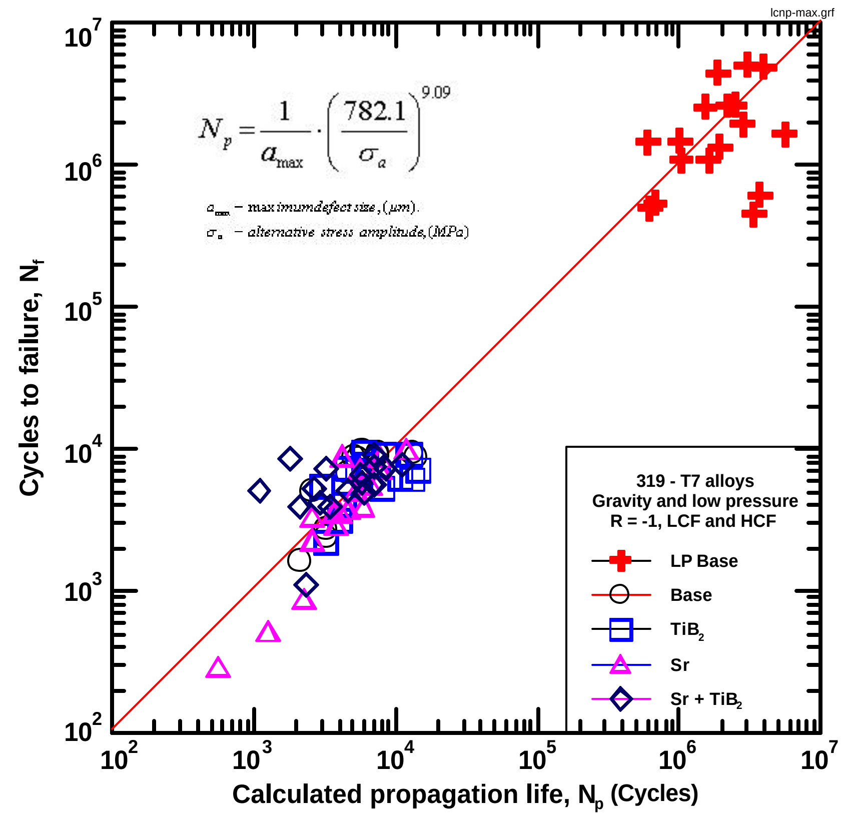

Microstructure Tolerant Design (MTD)

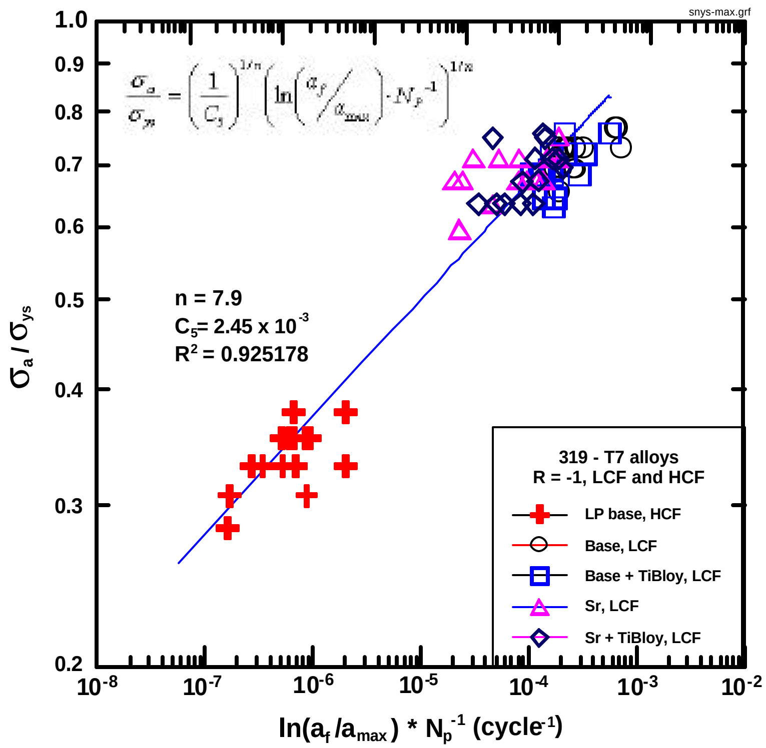

Short crack models

$$N_p = C \cdot \left(\frac{s_{ys}}{s_a} \right)^n \cdot \ln\left(\frac{a_f}{a_i} \right)$$

$$N_p = C' \cdot \left(\frac{s_{ys}}{e_{\max} \cdot s_a} \right)^n \cdot \ln\left(\frac{a_f}{a_i} \right)$$

(M.J. Caton *et al*., Met. Trans. 1999)

For applications

$N_f < 10^7$ cycles

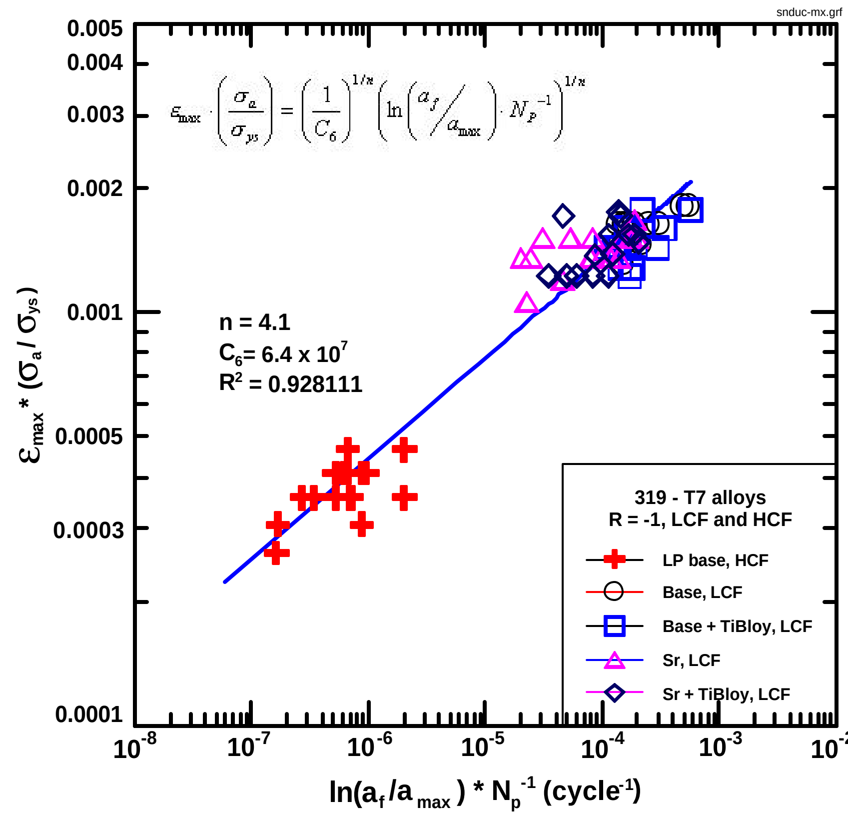

Comparison of Microporosity as Observed Metallurgically and in a SEM

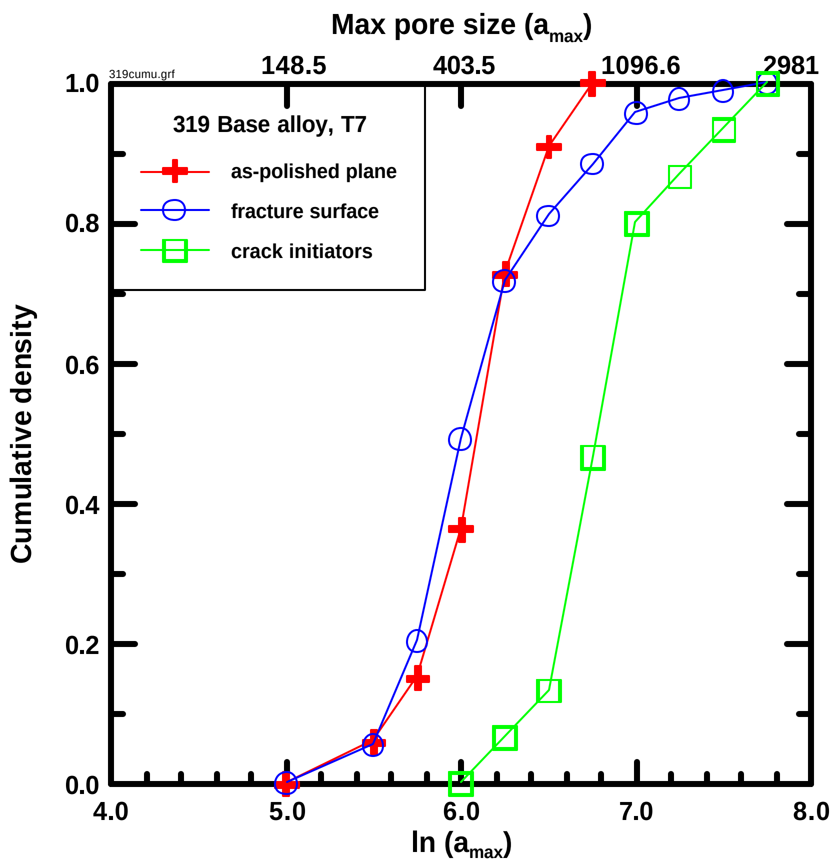

Gas Porosity

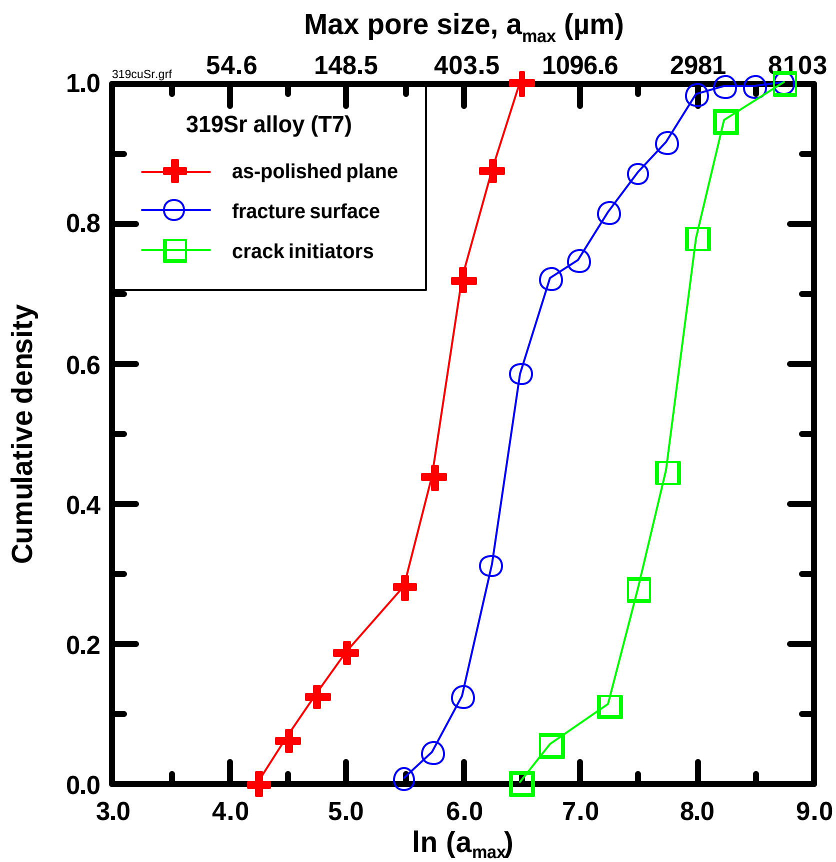

Shrinkage Porosity

Comparison of Microporosity as Observed Metallurgically and in a SEM

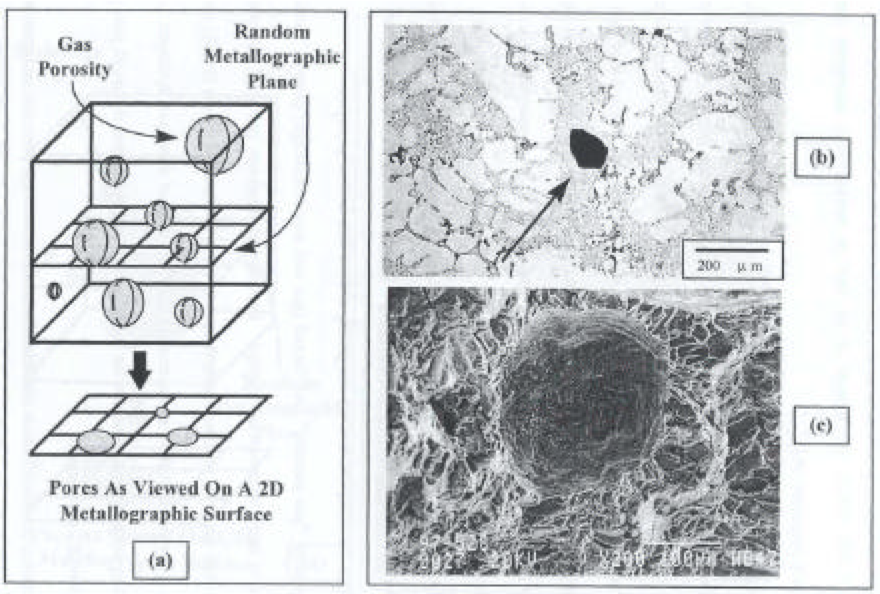

Gas Porosity

(J.M. Boileau, 2000)

Shrinkage Porosity

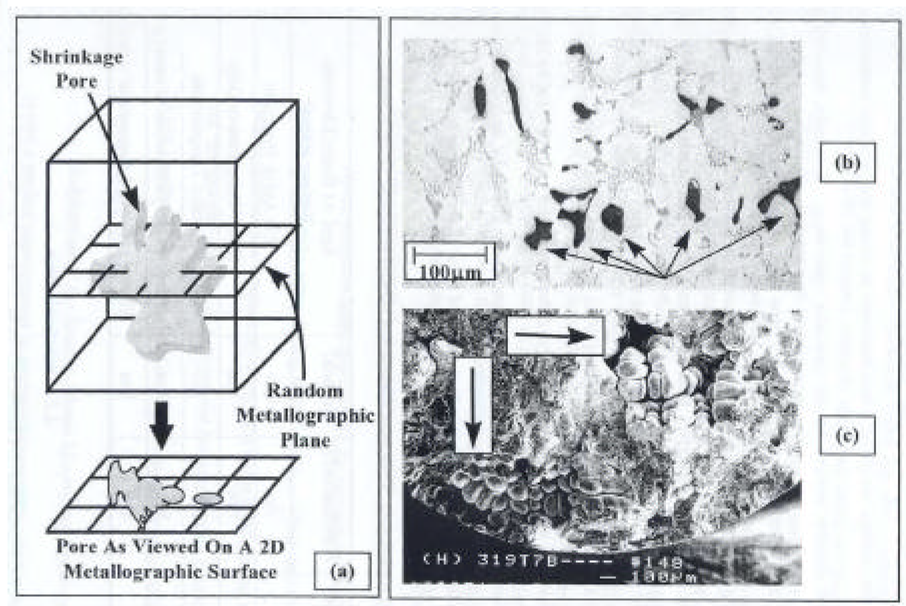

Extreme Value Statistics (EVS)

$$F(x) = \exp\left(-\exp\left(-\frac{x-l}{d}\right)\right)$$

x – pore size, l, d - EVS scale parameters

$$T = \frac{V}{V_0} \qquad T_b = T * 1000$$

(Murakami, *et al*, 1994, 97)

$$T = \frac{V}{V_0} = \frac{3.7\times10^6}{100} = 3.7\times10^4$$

$$T_b = 3.7\times10^4 \times 1000 = 3.7\times10^7$$

Alloys	Maximum defect size (μm)		
	As-polished	Fracture surface	EVS estimation
	(mean ± 3σ)	(mean ± 3σ)	(mean ± 3σ)
LP Base	167 ± 316	1573 ± 1645	1594 ± 560
Base	445 ± 477	968 ± 1210	2646 ± 1072
TiB_2	368 ± 402	1104 ± 944	2231 ± 1034
Sr	391 ± 400	2483 ± 3342	2246 ± 1030
SR + TiB_2	415 ± 467	2027 ± 1816	2562 ± 1136

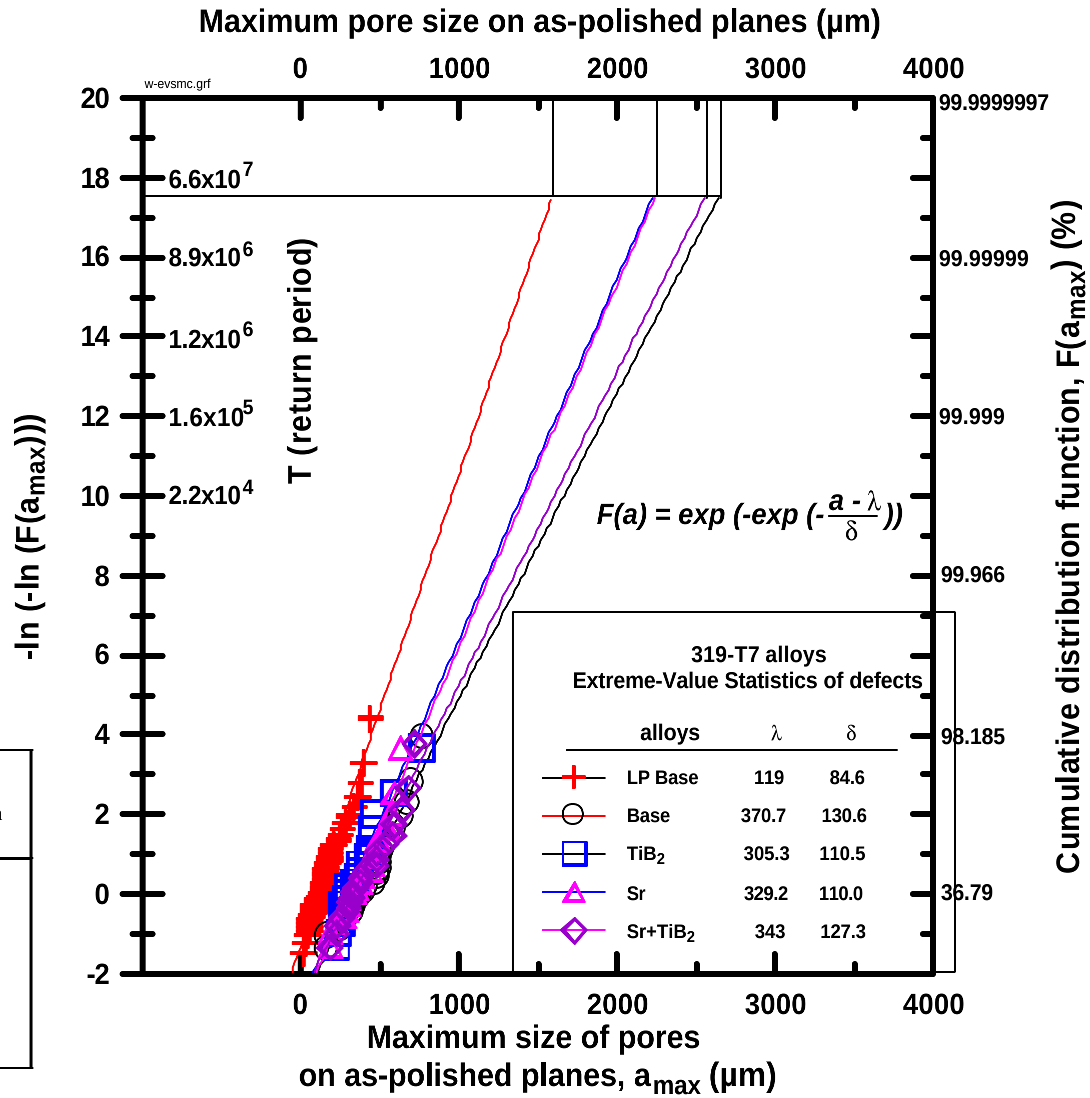

Application of Fracture Mechanics and EVS

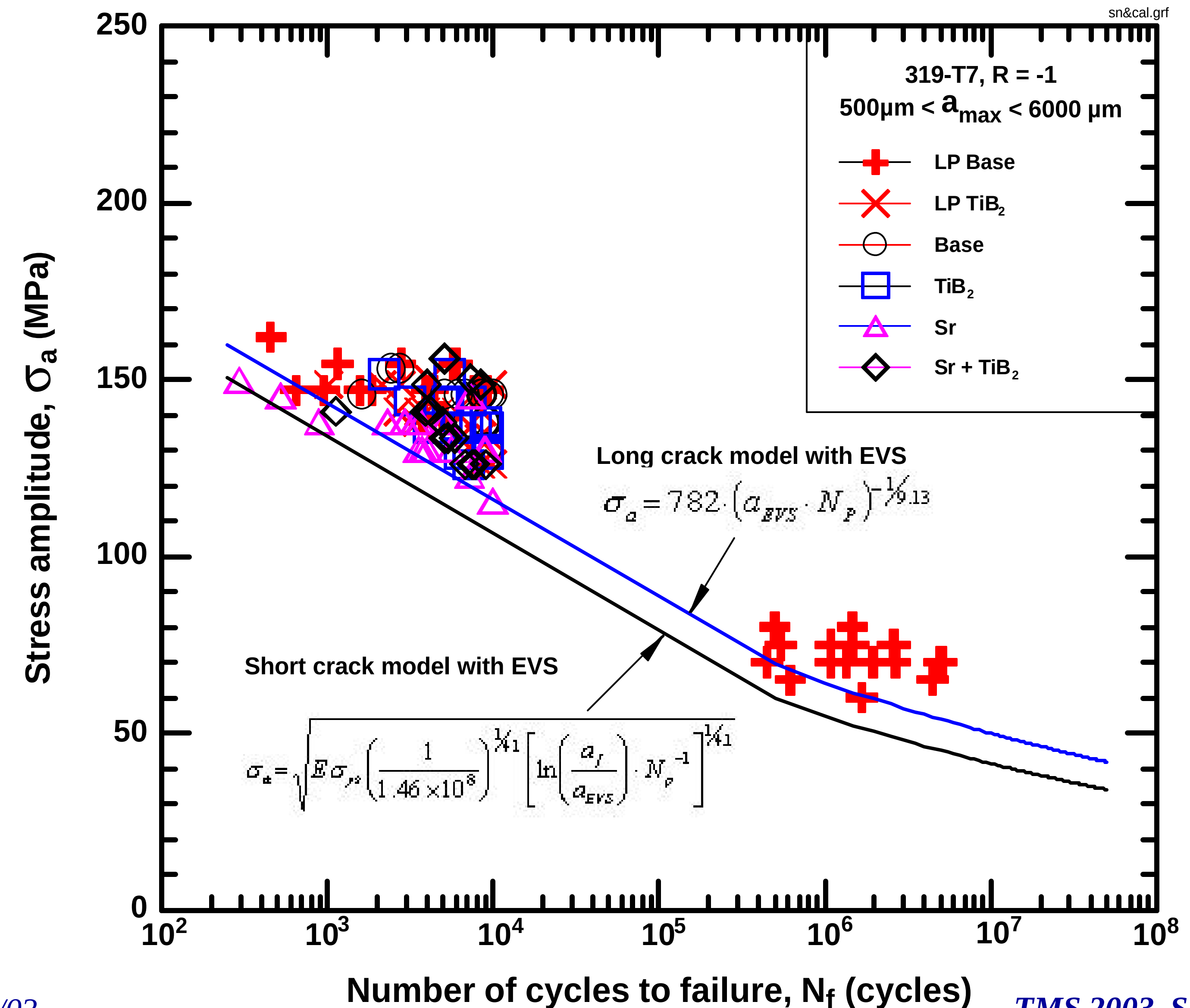

Summary and Conclusions

- Porosity plays the most important role in determining fatigue resistance. Compared with porosity, eutectic structure and intermetallic phases play a minor role in crack initiation. However, they can influence crack propagation rates late in life.
- Strontium modification of eutectic Si leads to macrosegregation of Cu-rich and Fe-rich intermetallic phases, and increases microshrinkage porosity.
- Compared with conventional gravity pouring, low pressure filling appears beneficial. It significantly reduced the volume fraction of porosity and increased tensile and fatigue strengths.

Summary and Conclusions

- The effect of grain refinement using "TiBloy" additions on microstructure and mechanical properties is marginal. It showed no significant benefit in unmodified (Sr-free) alloys. In Sr-modified alloys, TiBloy additions slightly reduce the volume fraction and size of porosity as well as the degree of intermetallic phase segregation, leading to a slight improvement in fatigue performance compared to Sr-modified material. The gains do not completely restore the strength of Sr-modified material to that of the base alloy.
- Fatigue cracks initially propagate mainly through the dendrites, leading to fewer eutectic (intermetallic) particles in the fatigue crack propagation region compared with tensile overload area.

Summary and Conclusions

- For the studied alloys with lives of ~10^6 – 10^7 cycles, the effective threshold stress intensity factor ($DK_{eff,\ th}$) is about 1MPa√m. For stress and defect combinations exceeding a stress intensity factor of 1MPa√m, the fatigue crack would initiate from the largest pores located at the free surface of the materials.
- Fatigue life can then be predicted using both long crack (LEFM – linear elastic fracture mechanics) and short crack (CTOD – crack-tip opening displacement) models together with inherent material characteristics.
- The largest defect (pore) size in a cast component can be estimated using extreme-value statistics (EVS) applied to metallographic measurements of pore size. Maximum pore size prediction by EVS agrees quite well with measurements of the initiation pore sizes from the fracture surface.